Contactless Fingerprint Identification using Level Zero Features

Ajay Kumar[1], *Yingbo Zhou*[1, 2]
[1]Department of Computing, The Hong Kong Polytechnic University, Hong Kong
[2]Department of Computer Science and Engineering, University at Buffalo, SUNY Buffalo, NY, USA
Email: *ajaykr@ieee.org*, *yingbo.zhou@ieee.org*

Abstract

Several recent research efforts in the biometrics have focused on developing personal identification using very low-resolution imaging resulting from widely deployed surveillance cameras and mobile devices. Identification of human faces using such low-resolution imaging has shown promising results and has shown its utility for range of applications (surveillance). This paper investigates contactless identification of such low resolution (~ 50 dpi) fingerprint images acquired using webcam. The acquired images are firstly subjected to robust preprocessing steps to extract region of interest and normalize uneven illumination. We extract localized feature information and effectively incorporate this local information into matching stage. The experimental results are presented on two session database of 156 subjects acquired over a period of 11 months and achieve average rank-one identification accuracy of 93.97%. The achieved results are highly promising to invite attention for range of applications, including surveillance, and sprung new directions for further research efforts.

1. Introduction

Tremendous growth in the demand for the automated and unconstrained human identification has evolved several common challenges for the next generation biometrics systems. Identification of humans from very low resolution images, such as those acquired from CCTV video and remote surveillance, has been of high interest in digital forensics and law enforcement applications. While investigating the suspects, law enforcement staff often comes across low-resolution biometrics images acquired at-a-distance. Low-resolution biometrics images have shown to be useful in personal identification using gait recognition [1], hand geometry, and also for the face recognition [4]. While the gait and hand geometry identification primarily employs the features extracted from the silhouette images, face recognition effectively employs the grey-level information in the low-resolution images. Some of the most promising work in very low resolution biometrics identification has been demonstrated for the face recognition. Several studies on the human face recognition have shown that a minimum resolution of somewhere between 32 × 32 to 64 × 64 pixels is needed for the face recognition from the most effective/popular algorithms [2]. However, even such resolution images may not be available from several common applications, *e.g.* CCTV networks from public streets or from remotely acquired images from standalone applications. Various super-resolution algorithms [3]-[4] have been shown to be effective for the face recognition from such very low resolution images.

The conventional fingerprint identification typically uses contact based imaging sensors that operate in a controlled environment. Such fingerprint image acquisition often results in partial or degraded images due to improper finger placement, accumulation of dirt, deformation of finger skin, sensor noise that builds up from the wear and tear of sensor surface coating. Therefore contactless fingerprint identification has been recently developed to provide faster, accurate and hygienic alternative to the existing approach [6]. As the research began to focus on remote and contactless biometric identification, low resolution imaging contents are now more important/common than ever before.

Table 1: Characterization of Fingerprint Features.

Level	Resolution*	Features
3	~ 1000 dpi	Pores, incipient ridges, etc.
2	~ 250 dpi	Minutiae features
1	~ 250 dpi	Ridge flow pattern/type
0	~ 50 dpi	Localized texture patterns

2. Our Work

Various features can be observed from the finger images acquired with different imaging resolutions. Three level characterizations of such features are quite popular in the fingerprint literature [5] and are summarized in table 1. The macro details of the fingerprints such as ridge flow and pattern types typically describe level 1 features. A minimum resolution of 250-300 dpi is typically required to extract such features from the standard algorithms. The contactless fingerprint† images acquired using very low

*Typical minimum/expected resolution for respective features

†Acquisition of digital finger surface images no longer require *printed inked impressions*. However due to the popularity of such terminology (fingerprint instead of finger images) in the literature, the low-resolution contactless finger images are also referred to as fingerprints in this paper.

resolution imaging, such as using webcam in this paper (~50 dpi, figure 1), does not illustrate clear details to estimate ridge/pattern flow (even after enhancement, figure 3) and therefore cannot extract level 1 features. The information content of such images essentially consists of broken line-like patterns representing creases and ridges

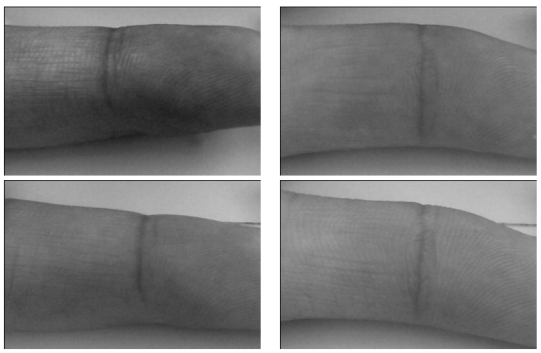

Figure 1: Each column images are from two different subjects but acquired in different imaging sessions.

of varying clarity. It is very difficult to establish the global uniqueness of such patterns, however their localized correlation with similar other neighbourhood line-like patterns can be exploited/explored for the personal identification. In the best of our knowledge, success of such localized matching scheme for very low resolution fingerprint images is yet to be investigated in the literature. However any success (partial or significant) from such an approach can have range of applications from digital forensics, indexing, to mobile and remote biometrics identification.

This paper investigates the problem of such contactless fingerprint identification using very low-resolution webcam imaging. We develop a completely automated approach for the extraction of potential region of interest, robust feature extraction and matching strategy that has shown to be highly effective in accommodating potential image variations from contactless imaging. In this context, we propose localized orientation of line-like features to extract stable finger surface features in the low-resolution imaging and present rigorous analysis to develop the matching strategy. Our experimental results on the database of 1566 images from 156 subjects, acquired over a period of 11 months, achieve highly promising results, *i.e.*, equal error rate of 0.32% and 3.95% from same session and two session images. In addition, our recognition results from 2 session database (156 subjects) achieve average recognition accuracy of 93.97%. These results should be interpreted in the context of very low resolution (~ 50 dpi) contactless imaging and are therefore of high significance. Our efforts to utilize such low resolution images and attempts to extract minutiae (-like) features, from the large number of spurious minutiae points, sprung new ideas and motivate new directions that invite further research efforts.

3. Image Acquisition and Preprocessing

The touchless[‡] imaging setup employed for the imaging is unconstrained. However, the user may fully or partially touch the finger dorsal surface with a white background that also illustrates preferred position/orientation for the imaging. The typical distance between the finger surface and the web camera is 5 cm. The webcam generates 640 × 480 pixels from 320 × 240 pixel image sensor and figure 1shows typical image samples from three subjects in our database.

The unconstrained fingerprint imaging employed in this work does not employ any special illumination. Therefore the presence of uneven illuminationand shadows in the acquired images results in the sharper contrast of upper finger boundaries than lower finger boundaries. Hence the upper finger boundary was selected for the fingerprint localization and segmentation. A Sobel edge detector followed by area thresholding is used to obtain the edge map and localize the finger boundaries. The resulting imageillustrates higher contrast and strong edge response from the upper finger boundaries. The slope of the resulting upper finger boundary is then estimated. This slope is used to automatically localize a fixed rectangular area which begins at a distance of 20 pixels from the upper finger boundary and is aligned along its estimated slope. We extract a fixed 400 × 160 pixel area, at a distance of 85 and 50 pixels respectively from the lower and right boundaries, from this rectangular region. This 400 × 160 pixel image is then used as the fingerprint image for the identification.

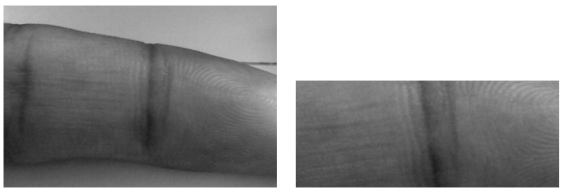

Figure 2: Acquired fingerprint image sample (left) and corresponding automatically segmented image (right).

3.1. Image Enhancement

The fingerprint image is firstly subjected to median filtering to eliminate the impulsive noise often present in the webcam acquired image. The resulting images have low contrast and uneven illumination. Therefore we firstly obtain the background illumination image from the

[‡]Touchless imaging avoids direct finger contact with sensor [5].

average of pixels in 10 × 10 pixels image sub-blocks and resize it back to the same dimension of the image using bicubic interpolation.

$$\bar{I}_M = \begin{cases} \frac{1}{\|W\|}\sum_{\forall(x,y)\in M} M(x,y), & \|W\| > 0 \\ 0 & Otherwise \end{cases} \quad (1)$$
$$W = \{\forall(x,y) \in M, \quad M(x,y) \neq I_{mg}\}$$

where M is the image sub block, W is the sub set of M that contains all the foreground pixels, *i.e.* those pixels whose values are not equal to the filled/fixed background pixel value, I_{mg} represents the background pixel intensity values while $\|\ \ |$ represents the cardinality operator that yields number of elements inside. The resulting image is subtracted from the median filtered fingerprint image and then subjected to histogram equalization. The image enhancement steps incorporated so far improves the amount of contrast and the effects of uneven illumination. However, they are not adequate to extract fingerprint details. Therefore the resulting image is subjected to unsharpening, *i.e.*, subtracting a Gaussian (σ =5, μ = 16) filtered image from the original image and then adding resulting image to the original image. It can be observed from the sample results from our database in figure 3 that the unsharpening has been quite successful in further improving the image contrast and texture details.

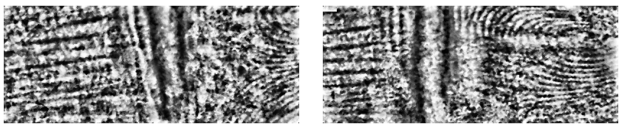

Figure 3: Two fingerprint image samples from one subject after enhancement.

4. Feature Extraction

As shown in figure 3,very low-resolution fingerprint images typically illustrate line-like structures and curves which suggest that the feature extraction approaches that can efficiently extract such localized information is likely to work well. Every pixel in such fingerprint image can be associated with a *dominant local orientation* which is likely to correspond with the coherence of the flow pattern in the original fingerprint. The localized Radon transform (LRT) and Gabor filter based extraction of such localized orientation flow is therefore expected to offer promising features for the identification and is therefore has been focus of our study [8]-[9]. We have investigated two such promising approaches for quantifying the observed features in contactless fingerprints. The matching strategy employed this work can account for high translation and rotational variations in the acquired images.The LRT of a discrete image $g[m, n]$ on a finite grid R_q^2 can be defined as:

$$s[L_\theta] = M_g(\theta) = \sum_{(x,y)\in L_\theta} g[x,y] \quad (2)$$

where $R_q = \{0, 1, \ldots, q-1\}$, q is a positive integer, and R_q^2 is centered at (x_0, y_0). The L_θ represents set of points on R_q^2 such that

$$L_\theta = \begin{cases} \{(x,y)|y = \tan(\theta) \times (x - x_0) + y_0, x \in R_q\}, & \theta \neq \frac{\pi}{2} \\ \{(x,y)|x = x_0, y \in R_q\}, & \theta = \frac{\pi}{2} \end{cases} \quad (3)$$

where $\theta \in [0, \pi]$ and denotes the angle between line L_θ and the positive x-axis, and L_θ is the line passing through the centre (x_0, y_0) of R_q^2 . The orientation of the line-like local patterns is estimated from the values of LRT and mathematically be represented as follows:

$$R_l(x_0, y_0) = \arg\{min_l(s[L_\theta])\}, \quad l = 1, 2, \ldots, D \quad (4)$$

where the $R_l(x_0, y_0)$ represents the estimated direction of pixel $g[x_0, y_0]$, and D represents the number of directions. This operation is repeated as the centre of lattice of R_q^2 moves over all the pixels in the image. At each position, the dominant orientation R_l is computed to form the feature vector of fingerprint image. The LRT is efficient in extracting line and curve segments in the local area. The key idea is that the curved lines can be estimated by small piecewise line segments and it integrates the intensity value in a local region in all defined orientations; but instead of integrating all the pixel values inside the local region, only the pixels that fall into the confined line width area is integrated, and the orientation that gives the maximum (or minimum depending on the feature) integration value is selected as the dominant direction. The image representation of extracted features, *i.e.*, feature map, illustrates that the line-like features the image are well presented, however, for the region that have highly curved lines the feature map is less representative.

Another approach for the estimation of such localized orientation is to employ a set of even Gabor filters to comparatively ascertain the maximum localized flow response and encode using its direction index. This approach is also referred to as CompCode approach and is detailed in reference [11]. In an attempt togenerate best possible performance from the fingerprint images, we rigorously evaluated various combinations of parameters (on training data) and report the corresponding results.

5. Generating Matching Scores

The matching scheme devised for the contactless fingerprint matching attempts compute the best matching scores between two images while accounting for possible spatial image shifts and rotations. These image variations are often caused by inaccurate (non-ideal) presentation of fingers in the imaging setup or due to the inaccurate localization and normalization. The matching scores

$\xi(R,T)$ between two binarized feature map R and T are generated as follows:

$$\xi(R,T) = \min_{\forall i\in[0,2w],\forall j\in[0,2h]}\left(\frac{\sum_{x=1}^{m}\sum_{y=1}^{n}\odot(\tilde{R}(x+i,y+j),T(x,y))}{\sum_{x=1}^{m}\sum_{y=1}^{n}(\tilde{R}(x+i,y+j)\oplus -1)}\right) \quad (5)$$

where m and n represent the width and height of the feature template respectively. The registered feature image is represented as $\tilde{R}$ with width and height expanded to $2w + m$ and $2h + n$, $\odot$ is Hamming distance operator, and $\oplus$ is the Exclusive OR operator that generates unity while two operands are different and zeros otherwise, while

$$w = floor\left(\frac{m}{t_w}\right),\ h = floor\left(\frac{n}{t_h}\right)$$

$$\tilde{R}(x,y) = \begin{cases} R(x-w,y-h), x\in[w+1,w+m\,], y\in[h+1,h+n] \\ -1, \quad Otherwise \end{cases} \quad (6)$$

where t_w and t_h are the constants introduced to control the translation distance in horizontal and vertical directions.

The matching score generated from the scheme in equation (5) represents global fingerprint texture image matching scores. However, the matching scores among the localized sub fingerprint texture regions (in two images) are more robust to rotations and local/partial distortions. Such localized matching scores should be more effectively accounted while matching low resolution fingerprint images. Therefore we also investigated a block-wise matching scheme which matches the corresponding sub-block of the fingerprint using equation 5 (referred to as the local scheme), which has shown to offer improved matching results and is evident from the experimental results presented in next section.

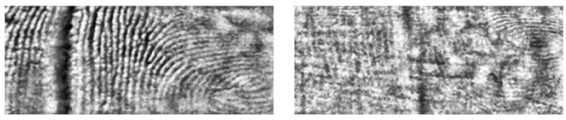

Figure 4: Enhanced fingerprint image samples from two different subjects.

6. Experiments and Results

In order to ascertain the performance improvement using the proposed schemes, we performed rigorous experiments on the acquired database as in the best of our knowledge there is no such database publicly available yet.

Database

The low-resolution fingerprint database employed in this work consists of 1,566 images acquired from 156 volunteers over a period of eleven months using the contactless imaging setup. The fingerprint images were acquired in two separate sessions with a minimum interval of one month, maximum interval of over six months and the average interval of 66.8 days. A total of 105 subjects turned up for the imaging during the second (time) session. In each session, 6 fingerprint image samples from the index finger of every subject were acquired.

The normalized and enhanced fingerprint images also illustrate rotational variations, as can be observed from image samples shown in figure 4. Observed rotational variations in fingerprint images are relatively large. Therefore to robustly address such variations, we enriched the training samples by including their rotated training samples at -6, -3, 3, and 6 degrees.

Experimental Results

The key objective in the first set of experiments was to ascertain the performance and the robustness of various algorithms when the fingerprint images from both sessions are employed. The time span between imaging sessions is likely to introduce variations in the images, mainly from temporal changes (if any, in fingerprint patterns) and/or pose variations resulting from unconstrained fingerprint imaging. Firstly, the six fingerprint images acquired during the first imaging session were employed to build up the training set while the corresponding 6 images acquired during the second session are used as testing/validating data to ascertain the performance. Therefore, the number of genuine score is 630 (105 × 6) and the number of imposter score is 65,520 (105 × 104 × 6) for each of the fingerprint matching.

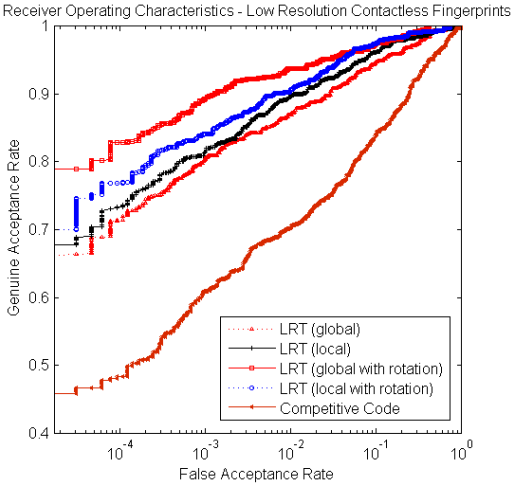

Figure 5: The ROC for authentication performance from contactless fingerprint images (two sessions).

Table 2: Comparative Performance (2 Sessions)

Approach	EER
LRT (global)	6.58%
LRT (local)	5.50%
LRT (global with rotation)	**3.95%**
LRT (local with rotation)	4.49%
CompCode	13.92%

The parameter D was fixed as 12 for all the experiments in this paper. The experimental results from various approaches (discussed in section 3-4) using equal error rate (EER) is summarized in table 2 and the receiver operating characteristics (ROC) for the corresponding performances is illustrated in figure 5.

The experimental results in table 2and figure 5 illustrates that the LRT based matching performs significantly better than *CompCode* which suggests its advantage in encoding line-like local features. The usage of these rotated training samples shows apparent performance improvement for both methods (about 20% in EER).

The next set of experiments were focused to ascertain low resolution fingerprint matching from same session but with relatively larger dataset using exhaustive cross validation. Therefore all the fingerprint images acquired in the first session, *i.e.* 156 subjects with 6 images per subject, were employed for the performance evaluation. The performance was firstly evaluated from 6-fold cross validation on the index finger images individually and the average of results (EER/ROC) is reported. Therefore, the total number of genuine score and imposter score is 936 (156 × 6) and 145,080 (156 × 155 × 6) respectively. The CompCode approach generates inferior performance (table 2) and was therefore not considered in further experiments. The experimental results from various approaches using EER is summarized in table 3.

Table 3: Comparative Performance (1 Session)

Approach	EER
LRT (global)	1.18%
LRT (local)	1.39%
LRT (global with rotation)	**0.32%**
LRT (local with rotation)	0.86%

In addition to the verification experiments, we also performed the experiments to ascertain the fingerprint recognition performance in more realistic scenario. We employed all the dataset acquired from 156 subjects for the recognition experiments. The dataset from 156 subjects in which the gallery was built up by the first session data of the 105 subjects, who contributed to both data sessions while the probe was composed by the corresponding 105 second session data along with the images from the rest [§] of 51 subjects. Therefore the recognition experiments had an additional class, *i.e.* not enrolled/identified. We employed the best performing authentication approach (table 2-3) for recognition experiment. Our experiments achieved average rank-one recognition accuracy of 93.97% and the corresponding CMC characteristics is shown in figure 7. The performance from recognition experiments considering two session data and 51 imposter subjects is highly promising.

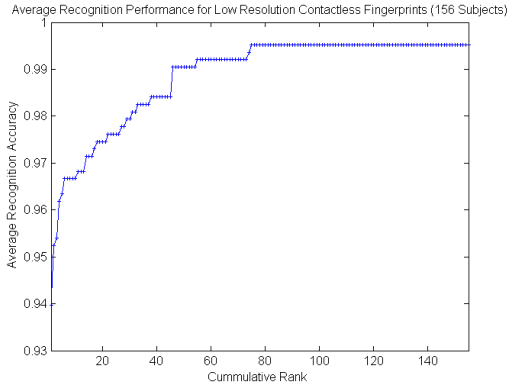

Figure 6: The CMC for recognition performance from contactless fingerprint images (two sessions).

7. Discussion

Human fingers are highly curved 3D surfaces and therefore the appearance of the fingerprint images can significantly vary with the view angle and illumination. The contactless presentation of fingers can significantly change the appearance of fingerprints, depending on the direction, illumination, distance from the camera and pose of the presented fingers. Furthermore, the appearance of the fingerprints can itself vary dramatically even within a single image (*e.g.* figure 4, *i.e.* some portions of the fingerprint image details are more clearly visible from the portions of 3D finger surface that receives more oblique illumination). The effectiveness of this robust performance from these finger texture images can be attributed to the steps of image normalization, boundary extraction, rotational alignment, robust feature extraction and importantly the matching strategy which can further minimize the influence of resulting scale and rotational variations in the presented fingers for imaging.

Fingerprint images are conventionally characterized by the minutiae based representation. Such representation does not utilize discriminatory texture information and can limit the matching of fingerprint images containing unregistered minutiae. Therefore Jain *et al.* [7] have suggested *FingerCode* based feature representation for fingerprint images. Such fixed length *FingerCode* represents the texture flow pattern of ridges and valleys from region of interest that tessellates around a reference points. Such an approach requires fingerprint images with (high) sufficient resolution, to accurately extract the fingerprint reference point and ridge flow pattern, and

[§]We estimated more realistic performance by using 51 subjects images, from the first session, as unknown identities.

therefore cannot be employed for very low resolution fingerprint images with ~ 50 dpi considered in this work. Another texture based matching of fingerprints using correlation plane energy and Fourier features has been detailed in [12] and [14] respectively. However this approach requires (and uses) high resolution or conventional fingerprint images to generate global matching scores and is not suitable for matching low-resolution fingerprint employed in our work. Absence of clarity between the (occasionally appearing, figure 4) ridge boundary is the prime for our failure to build up (lost) ridge pattern from such very low resolution images using popular fingerprint image enhancement approaches (*e.g*. as in [13]).

The fingerprint features that can be observed /extracted from the very low resolution imaging (~ 50 dpi) have been designated as *level 0* features in table 1. This term, *i.e*., level 0 features, is appropriate as the resolution of the images is much smaller than those required for level 1 features and the fact that it is the only the available integer below one.

8. Conclusions

This paper has investigated contactless fingerprint identification using very low resolution fingerprint (~ 50 dpi) images [15] and developed completely automated approach for matching such very low resolution webcam images. The experimental results presented in this paper from the database of low resolution contactless fingerprintimages, from the 156 subjects,have been highly successful. We achieved average recognition accuracy of 93.97% and equal error rate of 3.95% from two session images. Single session performance for the authentication experiments is quite high, equal error rate of 0.32%, as expected since the temporal and pose variations are expected to be least in single session images.

The unconstrained fingerprint imaging employed in this work utilizes low resolution images with varying clarity and our attempts to extract stable minutiae features were not successful. Therefore we relied on extracting texture like features to achieve reliable identification and the rigorous experimental results presented in section 6 suggest its promises. The extent of individuality of such level 0 features in very large populations is yet to be ascertained to compete and/or combine with more stable minutiae features employed in the conventional fingerprint identification. Despite possible reservation on the promises for large scale performance from such features, our experimental results have suggested that the investigated approach can be certainly useful for personal identification in small and medium size population, in addition to its promises in digital forensics. The promises from the experimental results presented in the paper from very low resolution fingerprint images has further encouraged us and sprung new directions for further research efforts. We are currently working to develop new mathematical models to extract true minutiae features from the pool of large (mostly false) minutiae features that can be extracted from some portions of very low resolution fingerprint images.

9. Acknowledgment

This work is supported by the competitive research grant from The Hong Kong Polytechnic University (2010-2011), grant number A-PK44 (PolyU 5181/10E).

References

[1] B. Bhanu and J. Han,*Human recognition at-a-distance in video*, Springer, 2010.

[2] Y. M. Lui, D. Bolme, B. A. Draper, J. R. Beveridge, G. Givens, and P. J. Phillips, "A meta-analysis of face recognition covariates," *Proc. BTAS'2009*, Sep. 2009.

[3] R. Abiantun, M. Savvides, B. V. K. Vijaya Kumar, "How low can you go? Low resolution face recognition study using kernel correlation feature analysis on FRGC v2 dataset," *Proc. Biometrics Symposium*, 2006.

[4] W. W. Zou and P. C. Yuen, "Very low resolution face recognition problem," *Proc. BTAS'2010*, Washington D.C., Sep. 2010.

[5] A. K. Jain, Y. Chen and M. Demirkus, "Pores and Ridges: High resolution fingerprint matching using level 3 features," *IEEE Trans. Pattern Anal. Mach. Intell.*, vol. 29, pp. 15-27, Jan. 2007.

[6] G. Parziale, "Touchless fingerprinting technology," *Advances in Biometrics: Sensor, Systems, and Algorithms*, N. K. Ratha and V. Govindaraju (*Eds*), Dec. 2007.

[7] A. K. Jain, S. Prabhakar and L. Hong, "A Multichannel Approach to Fingerprint Classification," *IEEE Trans. Pattern Anal. Mach. Intell.*,vol.21, no.4, pp. 348-359, April 1999.

[8] A. Kumar and Y. Zhou, "Human identification using KnuckleCodes," *Proc. BTAS'2009*, pp. 147-152, Washington DC, Sep. 2009.

[9] W. Jia, D.-S. Huang and D. Zhang, "Palmprint verification based on robust line orientation code," *Pattern Recognition,* vol. 41, no. 5, pp. 1504-1513, May, 2008.

[10] S. Z. Li, B. Schouten and M. Tistarelli, "Biometrics at a distance: Issues, Challenges and Prospects," *Handbook of Remote Biometrics*, Springer 2009.

[11] A. W. K. Kong and D. Zhang, "Competitive coding scheme for palmprint verification", *Proc. 17th ICPR*, Washington, DC, pp. 1051-4651, 2004.

[12] C. Watson and D. Casasent, "Fingerprint matching using distortion-tolerant filter,"*in Automatic Fingerprint Recognition Systems*, N. K. Ratha and R. Bolle (*Eds*), pp. 249-262, Springer, 2004.

[13] L. Hong, Y. Wan and A. K. Jain, "Fingerprint image enhancement: algorithms and performance evaluation," *IEEE Trans. Pattern Anal. Mach. Intell.*, vol. 20, pp.777-789, Aug. 1998.

[14] S. Chikkerur, C. Wu, and V. Govindaraju, "A systematic approach for feature extraction in fingerprint images,"*Proc. ICBA*, pp. 344-350, 2005.

[15] The Hong Kong Polytechnic University Low-Resolution Fingerprint Database, Version 1.0, 2010 http://www.comp.polyu.edu.hk/~csajaykr/fplr.htm